

Nanoscale Microstructure Formed During Crystallization and Shape Memory Behavior in Sputter-Deposited Ti-rich Ti-Ni Thin Films

J. Sakurai*, H. Hosoda*, S. Kajiwara** and S. Miyazaki*,#

* Institute of Materials for Metals, University of Tsukuba, Tsukuba 305-8573, Japan

**National Research Institute for Metals, 1-2-1 Sengen, Tsukuba 305-0047, Japan

It was found that unique microstructures consisting of nanoscale crystals and plate precipitates are formed in sputter-deposited Ti-rich Ti-Ni shape memory alloy thin films during the process of crystallization when the films were amorphous in the as-sputtered condition. In the crystallization process in an amorphous Ti-48.2at%Ni thin film, nanocrystals of B2 phase were formed by heat-treatment at about 670K. The diameter of the nanocrystals is about 10-50nm. During the formation of nanocrystals, surplus Ti atoms concentrate on the boundaries between nanocrystals, resulting in the formation of plate precipitates which locate along one of $\{100\}_{B2}$ planes and possess Ti atoms more than those in the amorphous condition. The Ti-rich thin plate precipitates improve the shape memory characteristics, achieving the shape recovery strain of about 6%. The microstructure varies as the heat treatment temperature increases; the thin plate precipitates turn to Ti_2Ni precipitates which are of semi-coherent with the B2 matrix. Similar observation was performed in other Ti-rich Ti-Ni thin films with different Ti concentration in order to investigate the effect of nominal Ti-concentration on the microstructure after crystallization at various temperatures.

Key words: Ti-Ni, sputter-deposition, shape memory effect, thin film, nanocrystal

1. INTRODUCTION

The development of the sputter-deposited Ti-Ni thin films has been demanded from the initial stage of development of micro electro mechanical systems (MEMS) such as micromachines and microrobots, since the shape memory alloys generate actuation force and displacement more than ten times of those in other actuator materials [1]. Moreover, intrinsic disadvantage of shape memory alloys, that is the slow response due to the limitation of cooling rate, can be greatly improved by micro-size dimensions, because the surface/volume ratio of materials drastically increases in thin films so that cooling becomes more efficient. Therefore, Ti-Ni thin films have been expected to create new application fields in micro-scale fields as powerful microactuators for micromechanical systems without suffering from their intrinsic disadvantage of slow response.

Many investigations have been done for bulk Ti-Ni alloys whose composition ranges from 49.6 to 51at%Ni[2]. In this composition range, a single B2 matrix phase can exist in the equilibrium phase diagram of the binary Ti-Ni sys-

tem[3]. The Ti-Ni alloys become brittle when the alloy composition is apart from the both sides of the alloy composition range to Ti-rich and Ni-rich regions, respectively, because Ti_2Ni intermetallic compounds are formed along grain boundaries in the Ti-rich region while $TiNi_3$ intermetallic compounds are formed in grains. Therefore, bulk Ti-Ni alloys with excess Ti or Ni have not been used for applications. However, the microstructure of sputter-deposited Ti-rich Ti-Ni thin films consist of plate precipitates and is different from that of bulk alloys. The plate precipitates locate along $\{100\}_{B2}$ planes and improve the shape memory characteristics[1, 4, 5]. It is conceivable that the microstructure and shape memory characteristics may be different in Ti-rich Ti-Ni alloy thin films if the alloy content varies. In order to understand the effect of alloy content on the microstructure and shape memory characteristics, Ti-rich Ti-Ni alloy thin films with two types of alloy contents were investigated in the present paper.

2. EXPERIMENTAL METHOD

Ti-rich Ti-Ni Thin films have been made by r.f. magnetron sputtering method using a Ti-50.0at%Ni target of 10cm in diameter. The films are deposited on glass sub-

Corresponding author. Fax: +81-298-55-7440.
e-mail: miyazaki@ims.tsukuba.ac.jp (S. Miyazaki)

strates in Ar atmosphere and their thickness was about 7-10nm. The substrate was not heated so that as-sputtered thin films are of amorphous. The films with different alloy compositions were prepared by changing the number of small pure Ti plates placed on the Ti-Ni target. The alloy compositions of the films were determined by the electron probe microanalysis (EPMA) to be Ti-48.2at%Ni and Ti-45.4at%Ni, respectively. The specimens were annealed at temperatures ranging from 663K to 973K for 3.6ks, respectively. Transformation temperatures were determined by a differential scanning calorimeter (DSC). Shape memory behavior was measured by constant load tests during thermal cycles. The microstructure was observed by transmission electron microscope (TEM) and X-ray diffractometer (XRD). The specimens with a disc shape of 3mm in diameter for TEM observation were prepared by electron polishing using CH_3COOH -10% HClO_4 electrolyte.

3. RESULT AND DISCUSSION

3.1 Microstructure

Shape memory characteristics are affected by microstructure of the specimen. A typical microstructure observed in a Ti-48.2at%Ni thin is shown in Fig. 1, which shows a HREM image at R.T. The Ti-48.2at%Ni thin film was annealed at 745K for 3.6ks. Ti_2Ni precipitates can not be seen, but white line contrasts of plate precipitates parallel to each of $\{100\}_{\text{B}_2}$ planes can be seen as indicated by an arrow in Fig. 1(a). An enlarged section of Fig. 1(a) revealed that the plate precipitates consist of a few atom planes and have not been observed in bulk specimens. Figure 1(b) shows an electron diffraction pattern taken from the area of Figs. 1(a). The zone axis of the electron diffraction pattern corresponds to $[001]_{\text{B}_2}$. Extra $1/3$ spots

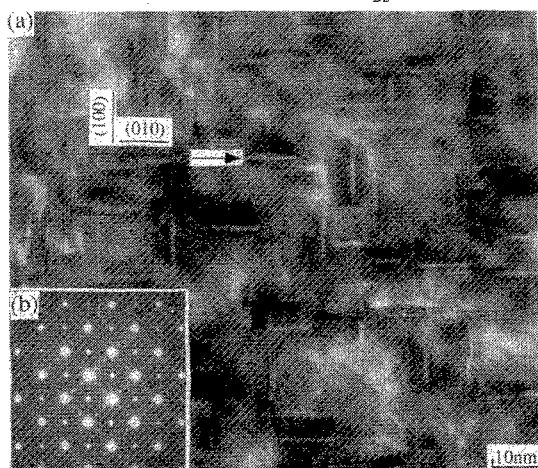


Fig. 1(a) High-resolution electron micrograph of a Ti-48.2at%Ni thin film heat-treated at 745K for 3.6ks and (b) the corresponding diffraction pattern.

along $[110]_{\text{B}_2}$ directions can be seen due to the rhombohedral phase (R-phase) at room temperature. Streaks along $\langle 100 \rangle_{\text{B}_2}$ directions can be seen in Fig.1(b). They correspond to the plate precipitates, because the thin plate precipitates lie on $\{100\}_{\text{B}_2}$ planes. The precipitates have a body centered tetragonal (BCT). Their thickness is about 0.5-1.5nm.

It is considered that the plate precipitates were formed in the crystallization process of an amorphous Ti-48.2at%Ni thin film. During the crystallization process, nanocrystals of B2 phase were formed first. The size of these nanocrystals is about 20 nm. Several millions nanocrystals coalesced into a grain with a diameter of 1-2 mm. After the formation of the nanocrystals, surplus Ti concentrated in the boundary of nanocrystals and Ti-rich plate precipitates were formed on $\{100\}_{\text{B}_2}$ planes.

Figure 2 shows XRD profiles of B2 phase measured at 373K. If the diffraction peaks of Cu (specimen holder) and Si (standard sample powders) are eliminated, a broad and shallow peak is observed around 41 deg. in the film heat-treated at 673K, since the film is not crystallized. A sharp peak appears at around 42 deg. in addition to the broad and shallow peak in the film heat-treated at 687K, indicating that the film is partially crystallized. The peak at 42 deg. corresponds to the diffraction from $\{110\}_{\text{B}_2}$ planes. The XRD profile observed in the film heat-treated at 697K indicates that the film is perfectly crystallized. In the film heat-treated at 765K, Ti-rich plate precipitates were observed by TEM but can not be detected by XRD. The diffraction patterns from the Ti_2Ni are observed first in the film heat-treated at 823K, because the Ti-rich plate

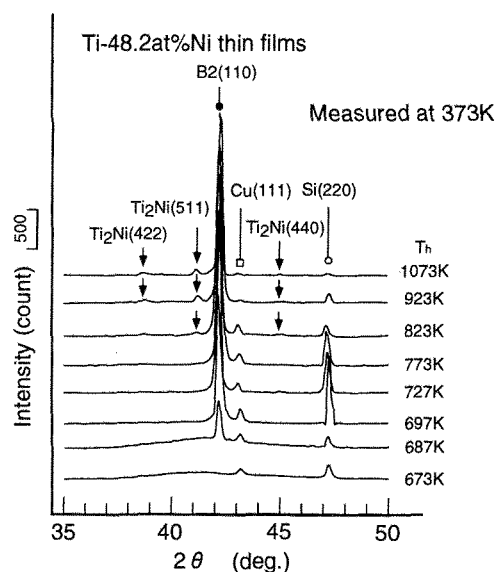


Fig. 2 Heat-treatment temperature dependence of X-ray diffraction profiles of the B2 phase measured at 373K in a Ti-48.2at%Ni thin film.

precipitates turned to Ti_2Ni precipitates which are semi-coherent with the B2 lattice.

TEM observation in Ti-45.4at%Ni films revealed that the Ti-rich plate precipitates were not formed during the crystallization process, because Ti_2Ni precipitates formed with random orientations in the amorphous at a temperature below the crystallization temperature. The B2 phase is formed when the film was heat-treated at a higher temperature. Since the Ti_2Ni precipitates are formed in the amorphous prior to the formation of the B2 phase, they are not semi-coherent with the B2 lattice in the Ti-45.4at%Ni.

3.2 Transformation temperatures

Shape memory effect occurs due to the martensitic transformation and its reversion. In the practical applications, the control of the transformation temperatures is very important. Figure 3 shows DSC curves of Ti-48.2at%Ni thin films with various heat-treatment temperatures, respectively. Since the film heated at 663K is amorphous, any transformation peaks cannot be seen. The film crystallized at 697K reveals two peaks corresponding to the R-phase transformation and its reversion upon cooling and heating, respectively. The characteristics of the R-phase transformation are such that the transformation strain and the transformation temperature hysteresis are less than 0.5% and only a few K, respectively, both of which are about one tenth of those of the martensitic transformation (M-phase). The transformation temperatures of the M-phase are too low to be observed by DSC. The film heat-treated at 973K shows two step B2-R-M transforma-

tions upon cooling and a single step M-B2 transformation upon heating. The film heat-treated at 1073K shows a single step B2-M transformation both upon cooling and heating.

Transformation temperatures of the Ti-45.4at%Ni films were also measured by DSC. They also showed similar heat-treatment temperature dependence; i.e., the R-phase transformation peak was observed in a film heat-treated at 697K, both R-phase and M-phase transformation peaks were observed in films heat-treated in an intermediate temperature region, and a single M-phase transformation peak was observed in a film heat-treated at 1073K. The transformation temperatures increase with increasing heat-treatment temperature both in Ti-48.2at%Ni and Ti-45.4at%Ni films. However, the transformation temperatures were lower in the Ti-45.4at%Ni films than in the Ti-48.2at%Ni in general except the films heat-treated at temperatures higher than 1073K.

3.3 Shape memory behavior

Shape memory behavior can be characterized by measuring the strain vs. temperature (S-T) relationship during thermal cycling (cooling and heating) under a constant load. Fig. 4 shows the S-T curves measured during thermal cycling under various constant stresses in a Ti-48.2at%Ni film heat-treated at 745K. The solid lines and dashed lines correspond to the S-T curves upon cooling and heating, respectively. The solid lines measured under a constant stress below 210MPa show two stage shape changes due to the R-phase and M-phase transformations, respectively. However, the solid lines measured under higher stresses show a single stage shape change due to the M-phase transformation. The R_s , R_p , M_s , M_p , A_s and A_f show the transformation temperatures, the capital letters R, M and A stand for the R-phase, M-phase and reverse M-phase transformations, respectively, while the subscripts s and f stand for the transformation start and finish, respectively. Shape recovery strain induced upon heating due to the reverse M-phase transformation is denoted by ϵ_A , while the permanent plastic strain is denoted by ϵ_p . If an applied constant stress becomes high enough, ϵ_p increases and ϵ_A decreases after reaching the maximum value. The critical stress for slip above which apparent ϵ_p starts to appear is denoted by σ_s .

The S-T curves of a Ti-45.4at%Ni film which was heat-treated at 873K were also measured under various constant stresses. The S-T curves measured under constant stresses below 400 MPa indicated two step shape changes due to the two step B2-R-M transformations upon cooling. The maximum stress below which two step transforma-

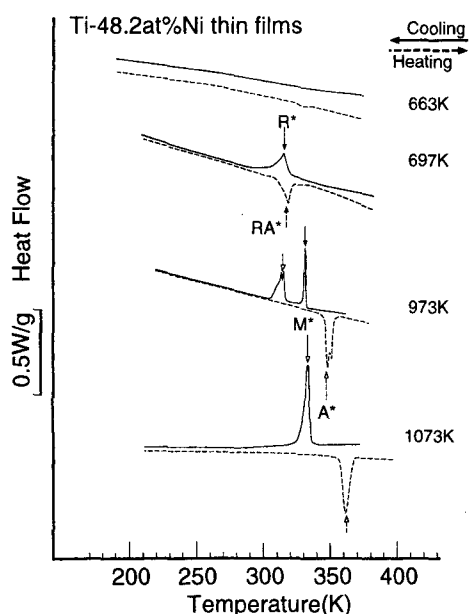


Fig. 3 DSC curves of Ti-48.2at%Ni thin films which were heat-treated at various temperatures.

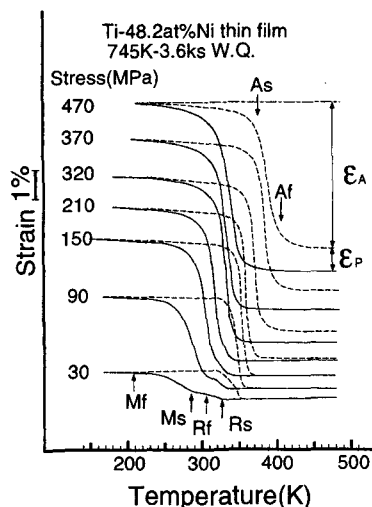


Fig. 4 Strain v.s. temperature curves measured during thermal cycling under constant stresses in Ti-48.2at%Ni thin films heat-treated at 745K for 3.6ks

tions occur is higher in the Ti-45.4at%Ni film than in the Ti-48.2at%Ni film, because the temperature range between R_s and M_s is wider in the former. The transformation strain of the former film is lower than that of the latter under any stresses.

The maximum recovery strain ϵ_A^{max} of both alloys is plotted as a function of heat-treatment temperature T_h alloys in Fig. 5(a). The maximum recovery strain increases with increasing T_h . After reaching the maximum value, the stress starts to decrease when T_h further increases. The maximum recovery strain is always higher in the Ti-48.2at%Ni than in the Ti-45.4at%Ni. The maximum of ϵ_A^{max} is only 2% for the former, while it amounts to 6% for the latter. Figure 5(b) shows the critical stress for slip, which is a measure of the stability of shape memory behavior, as a function of T_h . It decreases with increasing T_h and becomes insensitive to T_h . Since Ti_2Ni precipitates exist in the Ti-45.4at%Ni film more than in the Ti-48.2at%Ni film, the stress σ_s is higher in the former than in the latter.

4. CONCLUSIONS

The heat treatment temperature dependence of microstructure and shape memory characteristics were investigated in sputter-deposited Ti-rich Ti-Ni thin films and the following results were obtained.

(1) The amorphous films of Ti-48.2at%Ni heat-treated at near the crystallization temperature revealed a unique microstructural development, where nanocrystals were formed and coalesced into a single grain of 1-2 nm in diameter. During the crystallization process, surplus Ti atoms concentrate on the boundaries between

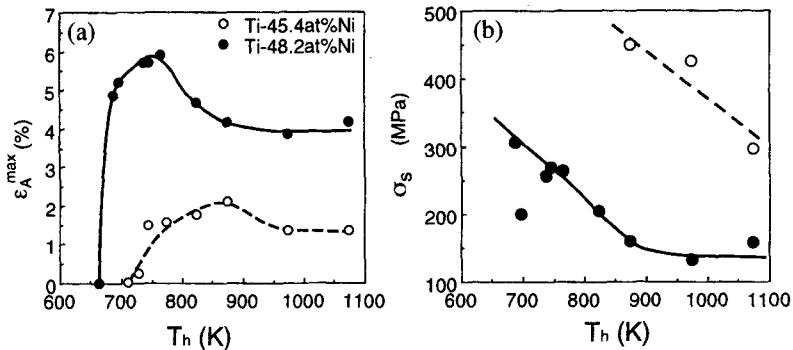


Fig. 5 Effect of annealing temperature on (a) the maximum recoverable strain ϵ_A^{max} and (b) the critical stress for slip σ_s in Ti-rich Ti-Ni thin films.

nanocrystals, resulting in the formation of Ti-rich plate precipitates which lie on $\{100\}_{B2}$ planes. When the heat-treatment temperature is high enough, Ti_2Ni precipitates were formed by nucleating from the Ti-rich plate precipitates.

(2) The Ti-rich plate precipitates were not formed in the Ti-45.4at%Ni films, because Ti_2Ni precipitates were formed in the amorphous during the crystallization process followed by the crystallization of B2 matrix phase. The Ti_2Ni precipitates were not semi-coherent with the B2 lattice, since the B2 phase was formed later than them.

(3) The maximum recovery strain and critical stress for slip increased and decreased, respectively, with increasing heat-treatment temperature for both alloys, and they are always higher and lower in the Ti-48.2at%Ni than in the Ti-45.4at%Ni, respectively.

ACKNOWLEDGEMENTS

The authors are grateful to Dr. T. Kikuchi, Mr. K. Ogawa and Mr. T. Matunaga for the collaboration in the initial stage of this research. This work was supported by the Grant-in-Aid for Fundamental Scientific Research (Kiban B(1998), A(1999)) from the Ministry of Education, Science, Sports and Culture, Japan.

REFERENCES

- [1] S. Miyazaki and A. Ishida : *Materials Science and Engineering*, **A 273-275** (1999) 106-133.
- [2] S. Miyazaki and K. Otsuka: *ISIJ International*, **29** (1989) 353-377.
- [3] *Phase Diagrams of Binary Titanium Alloys* (ed. By J. L. Murray), ASM International, Ohio (1987) p. 197.
- [4] S. Kajiwara, T. Kikuchi, K. Ogawa, T. Matunaga and S. Miyazaki : *Phil. Mag. Lettlers*, **74** (1996) 137-144.
- [5] S. Kajiwara, K. Ogawa, T. Kikuchi, T. Matunaga and S. Miyazaki : *Phil. Mag. Lettlers*, **74** (1996) 395-404.